Identification of a novel N-terminal hydrophobic sequence that targets proteins to lipid droplets

John K. Zehmer, René Bartz, Pingsheng Liu and Richard G. W. Anderson*

Department of Cell Biology, University of Texas Southwestern Medical Center, Dallas, TX 75390-9039, USA

*Author for correspondence (e-mail: richard.anderson@utsouthwestern.edu)

Accepted 11 March 2008
Journal of Cell Science 121, 1852-1860 Published by The Company of Biologists 2008
doi:10.1242/jcs.012013

Summary

AAM-B is a putative methyltransferase that is a resident protein of lipid droplets. We have identified an N-terminal 28 amino acid hydrophobic sequence that is necessary and sufficient for targeting the protein to droplets. This sequence will also insert AAM-B into the endoplasmic reticulum (ER). A similar hydrophobic sequence (1-23) in the cytochrome p450 2C9 cannot substitute for 1-28 and only inserts AAM-B into the ER, which indicates that hydrophobicity and ER anchoring are not sufficient to reach the droplet. We found that a similar N-terminal hydrophobic sequence in cytochrome b5 reductase 3 and ALDI could also heterologously target proteins to droplets. Targeting is not affected by changing a conserved proline residue that potentially facilitates the formation of a hairpin loop to leucine. By contrast, targeting is blocked when AAM-B amino acids 59-64 or 65-70, situated downstream of the hydrophobic sequence, are changed to alanines. AAM-B-GFP expressed in *Saccharomyces cerevisiae* is also faithfully targeted to lipid bodies, indicating that the targeting mechanism is evolutionarily conserved. In conclusion, a class of hydrophobic sequences exists that when placed at the N-terminus of a protein will cause it to accumulate in droplets and in the ER.

Supplementary material available online at
http://jcs.biologists.org/cgi/content/full/121/11/1852/DC1

Key words: Organelle targeting, ER, Lipid droplet, Adiposome, Membrane traffic

Introduction

Lipid droplets are sites of triglyceride and cholesterol ester storage that in the past have been considered to be inert cell inclusions (Murphy, 2001). Recent proteomic analysis, however, suggests that droplets are specialized for managing lipid storage, processing and distribution within the cell. From yeast to man, the droplet appears to be rich in enzymes that catalyze the biosynthesis, storage and degradation of lipids, as well as in numerous proteins that regulate intracellular membrane traffic (Binns et al., 2006; Brasaemle et al., 2004; Fujimoto et al., 2004; Liu et al., 2004; Umlauf et al., 2004; Zweytick et al., 2000). We have proposed that the machinery responsible for lipid accumulation deserves special status as an organelle, and suggested the name adiposome for this cellular compartment. Thus, in response to an increase in cellular fatty acid or cholesterol, adiposomes package esterified lipids into droplets surrounded by a monolayer of phospholipid. In eukaryotic cells, the adiposome appears to be a subcompartment of the endoplasmic reticulum (ER) where esterified lipids accumulate in the middle of the bilayer and subsequently bud into the cytoplasm (van Meer, 2001). Virtually all eukaryotic and many bacterial cells can accumulate lipid droplets, which suggests that the adiposome machinery is common to all cells. All organelles contain core molecules that govern their biogenesis and function, as well as transient molecules that associate only under specific cellular conditions. Targeting to an organelle generally depends on the ability of core molecules to recognize specific conformational states present in the transient molecule. An important early goal for understanding adiposome biology, therefore, is to identify targeting motifs in proteins that direct them to this compartment.

A number of different droplet-associated proteins have been examined for targeting information. A dominant theme is that hydrophobic sequences appear to be important. One type of motif is the proline knot, a ~72 amino acid hydrophobic sequence found in the middle of plant oleosins. The proline knot is thought to direct the protein to the droplet from its site of insertion in the ER, leaving flanking hydrophilic residues in the cytoplasm. The flanking sequences may also participate in targeting through an interaction with phospholipids on the surface of the droplet (Abell et al., 2002). A similar proline knot has been identified in the core protein of the hepatitis C virus and shown to be necessary for targeting to lipid droplets (Hope et al., 2002). Caveolins also have a central 33 amino acid hydrophobic region that might be important for targeting to droplets (Ostermeyer et al., 2001). Hydrophobic sequences in Erg1p, Erg6p and Erg7p have also been implicated in targeting to yeast droplets (Mullner et al., 2004). Targeting of TIP47, a member of the PAT (perilipin, ADRP and TIP47) family of droplet-associated proteins, appears to depend on a C-terminal hydrophobic cleft (Ohsaki et al., 2006). Likewise, a hydrophobic region within perilipin (amino acids 242-260, H1; 320-342, H2; and 349-364, H3) controls targeting (Subramanian et al., 2004). In contrast to hydrophobic information, targeting of ADRP appears to depend on a hydrophilic helical region between amino acids 189 and 205 (McManaman et al., 2003) that does not overlap with the putative targeting regions in perilipin. The phosphatidylinositol (PI) transfer domain of Nir2 appears to use phosphorylation signals to target to droplets (Litvak et al., 2002). Nir2, which has been implicated in maintaining the proper level of diacylglycerol in the Golgi apparatus (Litvak et al., 2005), can either be in the Golgi apparatus or in the lipid droplet, depending on its phosphorylation state.

The monolayer of phospholipid that surrounds each droplet is likely to have a major influence on protein targeting to the organelle. We would expect, for example, that some resident

proteins might be specially adapted to span a single layer of phospholipid. Among the proteins we recently identified in a proteomic screen of isolated CHO K2 lipid droplets (Liu et al., 2004) was a putative methyltransferase potentially of the ubiquinone biosynthetic pathway called AAM-B [also known as methyltransferase-like 7B (METTL7B)]. AAM-B caught our attention because it had a single extreme N-terminal hydrophobic sequence similar to that which is found at the N-terminus of cytochrome p450 enzymes and is necessary for ER localization (Bracey et al., 2004). Using mutagenesis and expression in HeLa cells, COS7 cells and yeast, we find that this N-terminal hydrophobic 28 amino acid sequence is necessary and sufficient for targeting AAM-B to lipid droplets. The sequence just C-terminal to the hydrophobic region, however, can influence migration to the droplet without affecting insertion into the ER. The 28 amino acid sequence appears to possess special targeting properties other than simple hydrophobicity because a similar N-terminal hydrophobic sequence from cytochrome p450 2C9 (CYP2C9) was unable to target to droplets. Indeed, we found hydrophobic sequences in the droplet proteins ALDI and CYB5R3 that could also target. We conclude that a special class of hydrophobic sequences exists that when present at the N-terminal end of a protein will cause it to accumulate in droplets.

Results

The overall organization of AAM-B is shown in Fig. 1A (WT). The protein consists of the 28 amino acid hydrophobic domain (Fig. 1B, AAM-B), a 45 amino acid juxtamembrane region (JuxtaM), a central 110 amino acid segment (Fig. 1, dark-blue region) that is predicted by sequence homology to be a methyltransferase catalytic fold (Marchler-Bauer and Bryant, 2004), and a C-terminal 61 amino acid region of unknown function. To confirm that AAM-B is targeted to droplets, we transiently expressed in HeLa cells a cDNA encoding a C-terminal, Myc-tagged human AAM-B and localized the protein by immunofluorescence with α-Myc IgG. We observed two expression patterns (Fig. 2A). In the first pattern, all of the α-Myc IgG staining was in a rim surrounding Bodipy-positive (green) droplets (Fig. 2A3). The second pattern consisted of what appeared to be reticular ER staining in addition to rim staining around the droplet (Fig. 2A4). We confirmed that the reticular staining was

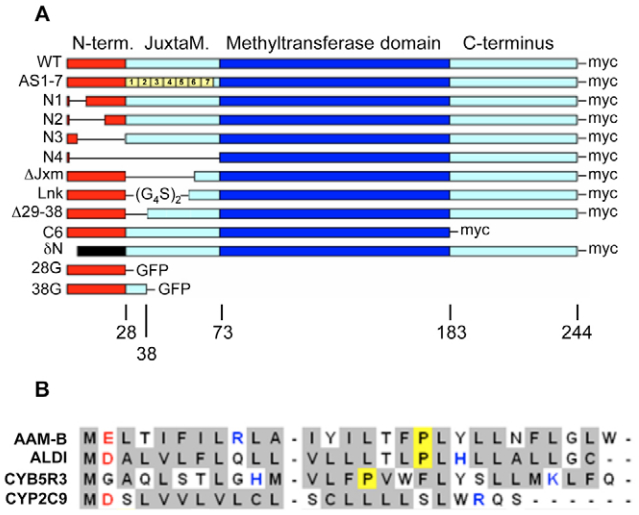

Fig. 1. The AAM-B constructs used in this study and alignment of the N-terminal hydrophobic regions of AAM-B, ALDI, CYB5R3 and CYP2C9. (A) Wild-type AAM-B (WT) has four domains: an N-terminal hydrophobic region, a putative juxtamembrane domain, a putative methyltransferase domain and a C-terminal region that lacks any distinguishing features. Deletions made in the various regions as well as three chimeric proteins used in this study are shown. Each diagram represents a single construct, with the exception of AS1-7, which is a summary of seven constructs: the seven numbered boxes represent the regions mutated to alanines in the corresponding seven constructs. (B) Alignment of the first 23-28 amino acids of AAM-B, its close homolog ALDI, CYB5R3 and the p450 family member CYP2C9. Shaded boxes highlight hydrophobic residues (amino acid value>0 on the Kyte-Doolittle scale). Acidic residues are in red, basic residues in blue and prolines are highlighted yellow.

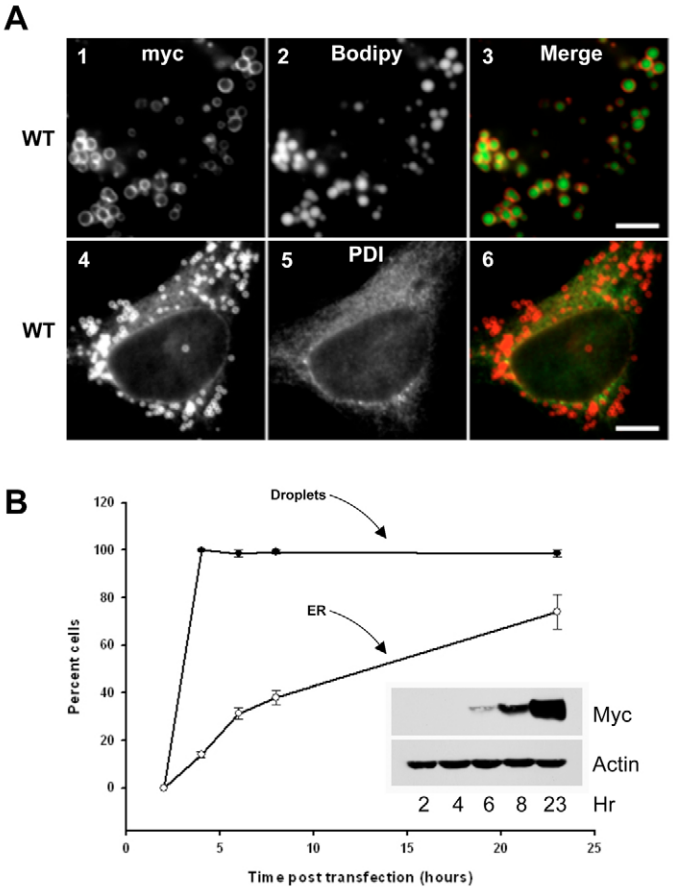

Fig. 2. AAM-B is targeted to droplets. (A) HeLa cells were transfected with cDNA encoding C-terminally Myc-tagged AAM-B and grown for 15 hours in media containing 100 μM oleic acid to induce lipid droplets. The cells were fixed and processed for indirect immunofluorescence localization of Myc (1,4) and protein disulfide isomerase (5) or stained for lipids with Bodipy 493/503 (2). Most cells had Myc staining (1) restricted to the periphery of neutral lipid-positive (2) droplets, as shown in the merge (3). Other cells displayed Myc staining (4) around lipid droplets and, in addition, a reticular pattern distributed throughout the cell that co-localized with α-PDI IgG (5), as shown in the merge (6). (B) HeLa cells grown on coverslips in the absence of oleate were transfected with cDNAs encoding wild-type, Myc-tagged AAM-B. At various times post-transfection, the cells on the coverslip were fixed and processed for immunofluorescence detection of Myc. The cells remaining in the dish were collected, lysed and processed for immunoblotting to detect Myc (inset). To quantify the distribution of AAM-B, images of stained cells were systematically acquired until 50 cells had been photographed for each time point. The cells were then scored for the presence of either lipid droplet alone, or droplet plus reticular ER staining patterns. We did not detect any expressing cells until after a 2 hour incubation. Each point is the average ±s.e.m. of three separate experiments. Scale bars: 5 μm.

ER by co-localizing the ER marker protein disulfide isomerase (PDI) (Fig. 2A5). This ER staining appeared to be more common in cells with only a few droplets, or in cells with the highest expression levels. We obtained similar results when we expressed AAM-B-Myc in normal rat kidney, CHO K2 and immortalized human fibroblast cells (data not shown).

To quantify these results, cells were transfected with a cDNA encoding AAM-B-Myc and grown for various times on coverslips in the absence of oleate (Fig. 2B). At the indicated time points, the cells on the coverslip were processed for immunofluorescence detection of AAM-B-Myc, while the cells remaining in the dish were processed for immunoblotting to monitor the expression level of AAM-B-Myc. The number of cells showing droplet staining and ER reticular staining was quantified as a function of expression time. Within 4 hours of transfection, immunofluorescence indicated the presence of expressing cells and nearly all these cells displayed only the droplet staining pattern (Fig. 2B, black circles). AAM-B-Myc was not detected by immunoblotting at this time (Fig. 2B, inset). As the expression level increased (inset), we saw progressively more cells displaying both droplet and ER staining patterns (white circles). Therefore, AAM-B appears to prefer droplets, but accumulates in the ER as the expression level in the cell increases.

The N-terminus is required for AAM-B localization to the droplet

The N-terminus of AAM-B consists of a hydrophobic core flanked by acidic and basic residues, similar to the N-terminal signal sequence/membrane anchors of p450 cytochrome family proteins (Fig. 1B). We therefore carried out experiments to determine the contribution of this region of the molecule to lipid droplet targeting. A series of deletions or substitutions was made (Fig. 1), the mutated proteins expressed in HeLa cells and localized by immunofluorescence. Removing the first nine (N1, not shown) or the first 18 (Fig. 3A-C, N2) amino acids had no effect on targeting to the droplet. By contrast, removing most of the hydrophobic portion of this region (amino acids 6-28) abolished targeting, and the protein appeared to be in bright-staining deposits in the cytoplasm (Fig. 3D-F, N3). To test whether other hydrophobic sequences could substitute for 1-28, we replaced this sequence of AAM-B with amino acids 1-23 of the cytochrome p450 CYP2C9 (Fig. 1, δN). This chimeric protein was found exclusively in the ER and did not co-localize with Bodipy-positive droplets (Fig. 3G-I). To determine whether wild-type AAM-B could recruit δN from the ER to the droplet, the two were co-expressed. Now δN co-localized with wild-type AAM-B in droplets (data not shown). The failure of δN by itself to target to droplets indicates that the N-terminal hydrophobic region of AAM-B contains information that is necessary for targeting to droplets.

The N-terminus of AAM-B is sufficient for targeting

We next searched for additional targeting information outside the hydrophobic N-terminus. We made a series of deletions of the C-terminus, the largest of which removed everything C-terminal to the methyltransferase domain (Fig. 1A, C6). Deletions of this region did not affect targeting to lipid droplets (supplementary material Fig. S1A-C). By contrast, deleting amino acids 29-61 in the putative juxtamembrane region (Fig. 1A, ΔJxm) completely abolished lipid droplet localization (Fig. 4A-C). Instead, the mutant protein exhibited an ER staining pattern (note the nuclear envelope) and it appeared to be aggregated.

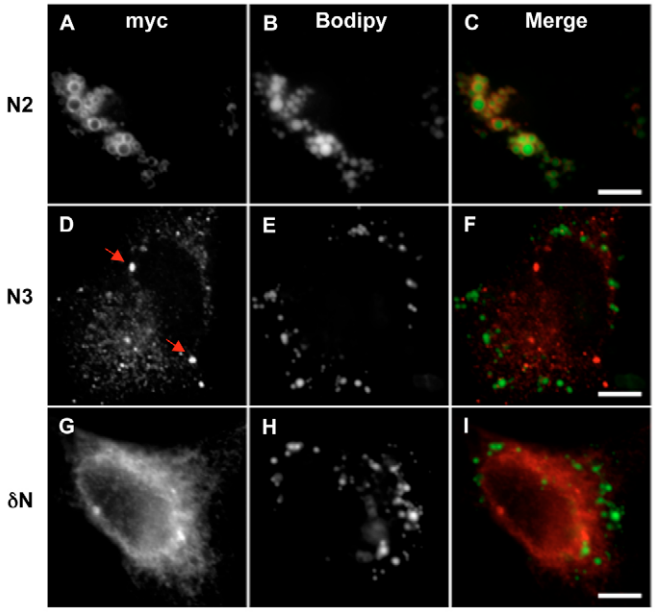

Fig. 3. Deletion of amino acids 6-28 interrupts AAM-B targeting to droplets. The indicated AAM-B mutants were expressed in HeLa cells and processed for immunofluorescence. (A-C) Deletion of amino acids 2-18 (N2) did not disrupt the targeting of AAM-B (A) to Bodipy 493/503-positive (B) lipid droplets (C). (D-F) AAM-B lacking amino acids 6-28 (N3) had a cytosolic distribution (D). Brightly staining regions (arrows) appear to be insoluble aggregates that do not overlap with Bodipy 493/503-stained (E) lipid droplets (F). (G-I) AAM-B with amino acids 1-23 of CYP2C9 substituted for amino acids 1-28 (δN) had a reticular pattern (G) that was not even weakly associated with Bodipy-positive (H) droplets (I). Scale bars: 5 μm.

To investigate the predicted juxtamembrane region further, we used alanine-scanning mutagenesis. Seven, Myc-tagged constructs were made, each with a six amino acid sequence of alanine residues replacing six amino acids of the putative juxtamembrane region (Fig. 1A, AS1-7). Collectively, these mutants cover amino acids 29-70. We expressed each construct in HeLa cells and determined their location by immunofluorescence. Substituting alanine for each of the first five sets of amino acids (Fig. 1, AS1-5) had no effect on targeting to droplets (for example, AS2, supplementary material Fig. S1D-F). By contrast, substituting alanine for regions 6 or 7 markedly reduced targeting to droplets and increased reticular ER staining (for example, AS6, supplementary material Fig. S1G-I). We noticed that, as in the case of the ΔJxm mutation, both AS6 and AS7 staining appeared punctate but in an ER pattern.

There are two principle ways to explain these results. One is that AS6 and 7 function as a positive signal for targeting to droplets, but getting there is dependent on the hydrophobic N-terminus. The other is that changes in the juxtamembrane region cause aggregation of the protein in the ER, thereby preventing it from reaching the droplet. To distinguish between these two possibilities, we attached different portions of the N-terminal region of AAM-B to GFP. When we fused the 1-28 hydrophobic region to the N-terminus of GFP (Fig. 1A, 28G) and expressed it in HeLa cells, the chimera targeted to droplets, but with low efficiency. A substantial amount of this chimeric protein displayed a reticular, ER pattern (Fig. 4D-F). If, however, we fused amino acids 1-38 of AAM-B to GFP (Fig. 1A, 38G), the construct targeted to droplets as efficiently as the wild-type protein (Fig. 4G-I). This suggests that amino acids 29-38 contain information that increases the efficiency of targeting. We

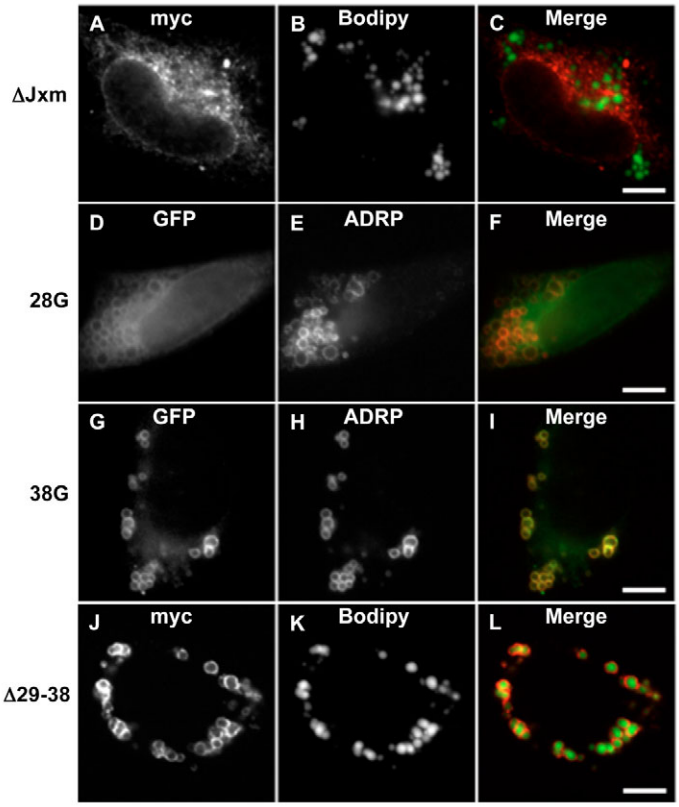

Fig. 4. Amino acids 1-28 are sufficient to target proteins to droplets. AAM-B mutants were expressed in HeLa cells and processed for immunofluorescence. (A-C) Deletion of amino acids 29-61 in the juxtamembrane region (A) disrupted targeting to Bodipy 493/593-positive (B) droplets (C). (D-F) GFP was fused to the C-terminal end of AAM-B amino acids 1-28 and expressed in HeLa cells. The chimera (D) was found in an ER pattern with some protein localized to ADRP-marked (E) droplets (F). (G-I) AAM-B amino acids 1-38 fused to GFP (G) co-localized with ADRP (H) on droplets (I). (J-L) Deletion of amino acids 29-38 from full-length AAM-B (J) did not influence targeting to Bodipy-positive (K) droplets (L). Scale bars: 5 μm.

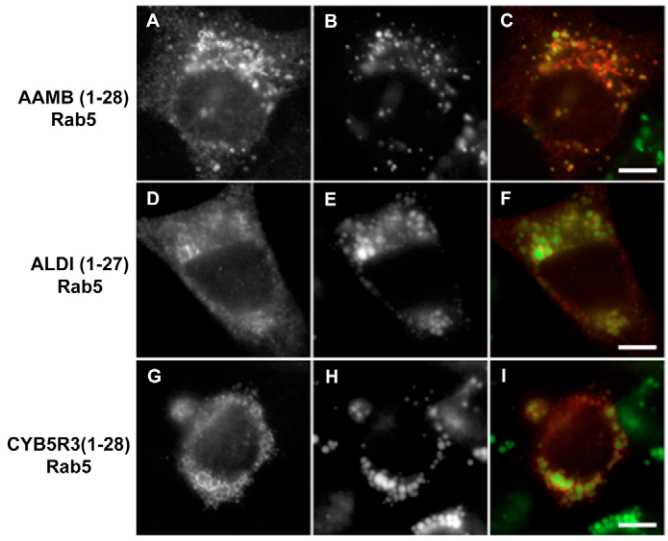

Fig. 5. N-terminal hydrophobic sequences from other droplet proteins are sufficient to target droplets. (A-C) Amino acids 1-28 from AAM-B fused to Rab5 S34N (A) target Bodipy-positive (B) droplets (C). (D-F) Amino acids 1-27 of mouse ALDI fused to Rab5 S34N were sufficient to target the protein (D) to Bodipy-positive (E) droplets (F). (G-I) Protein comprising amino acids 1-28 of CYB5R3 fused to Rab5 S34N (G) was also found surrounding Bodipy-positive (H) droplets (I). Scale bars: 5 μm.

then deleted amino acids 29-38 from full-length AAM-B (Fig. 1A, Δ29-38) and found that targeting to droplets was normal (Fig. 4J-L). We conclude that the juxtamembrane region (29-73) does not contain a positive signal for targeting to droplets but instead stabilizes AAM-B, allowing it to efficiently move to droplets.

The ability of the N-terminal 1-28 region of AAM-B to target proteins to droplets, whereas a similar hydrophobic region in CYP2C9 cannot, suggests that there is more information in the 1-28 region than simply hydrophobicity. To test this, we examined the lipid droplet targeting potential of two additional proteins that share with AAM-B an extreme N-terminal hydrophobic sequence (Fig. 1B). We chose to attach each hydrophobic region to a mutant, constitutively cytosolic form of Rab5. We speculated that these hydrophobic sequences might not work unless they were attached to another protein, and previously we found that 1-73 of AAM-B attached to Rab5 targets droplets correctly (Liu et al., 2007). Fig. 5A shows that AAM-B 1-28 targeted Rab5 to droplets. ALDI is another methyltransferase-like protein with substantial sequence similarity to AAM-B. Mouse ALDI contains a hydrophobic N-terminus similar to human AAM-B, and one study has shown that it will target to droplets (Turro et al., 2006). ALDI 1-27 also targeted to droplets, although targeting appeared to be inefficient (Fig. 5D-F). We also tested another protein with N-terminal hydrophobic regions, cytochrome b5 reductase 3 (CYB5R3), that we identified previously in the lipid droplet proteome (Liu et al., 2004). Amino acids 1-28 of CYB5R3 targeted Rab5 very efficiently to droplets (Fig. 5G-I). One notable feature in common among all the targeting-proficient hydrophobic sequences was the presence of a proline residue near the center of the sequence (Fig. 1B). However, substituting leucine for proline had no effect on targeting in any of these molecules (data not shown).

We next wanted to determine whether the AAM-B N-terminal targeting sequence worked in a more primitive cell. There are two proteins with sequences similar to AAM-B in *S. cerevisiae* but neither has a terminal hydrophobic region, and they are not in lipid bodies (Huh et al., 2003). We co-expressed the wild-type AAM-B-GFP with the lipid body marker Erg6-DsRed in the BY4742 haploid yeast strain (Fig. 6) (Binns et al., 2006; Hettema et al., 2000; Huh et al., 2003). The wild-type AAM-B-GFP (Fig. 6A,E) appeared as ring-shaped structures that co-localized with Erg6-DsRed (Fig. 6B,F). We conclude that AAM-B 1-28 will target to droplets in all eukaryotic cells.

We next explored the topological potential of the 1-28 hydrophobic sequence in AAM-B. The data so far suggest that AAM-B is anchored into the membrane by its hydrophobic domain, but this region could assume a number of different topologies. For example, it could form a hairpin loop in the outer monolayer of the droplet and the ER. Therefore, we fused GFP to the N-terminus of an AAM-B that had a C-terminal Myc tag and expressed it in HeLa cells. The GFP-AAM-B correctly targeted to droplets (data not shown). Membranes were isolated and treated either with buffer alone (Fig. 7A, lane 1), protease (lane 2) or protease plus protease inhibitor (lane 3), before processing for immunoblotting. Trypsin completely digested both the N-terminus (Fig. 7A, GFP, lane 2) and C-terminus (Myc) of AAM-B (lane 2), suggesting that both ends of the molecule are oriented towards the cytoplasm. The

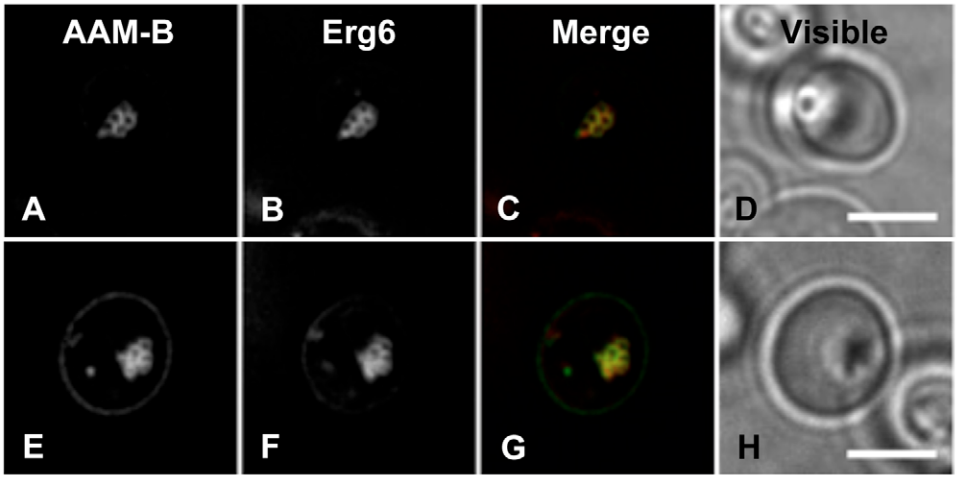

Fig. 6. AAM-B targets to yeast lipid droplets. Cells were co-transformed with AAM-B-GFP and Erg6-DsRed and grown on selective plates. AAM-B-GFP (A,E) co-expressed with Erg6-DsRed (B,F) co-localized (C,G) on *S. cerevisiae* lipid bodies (shown under light microscopy in D,H). Scale bars: 5 μm.

membrane remained intact during the treatment because we observed a ~10 kDa reduction in the size of calnexin (Cnx), which corresponds to the size of its cytoplasmic domain. Both proteins migrated on gels consistent with their normal molecular weight, both when untreated (lane 1) and when protease inhibitors were included with the protease cocktail (lane 3). These results suggest that the hydrophobic targeting sequence in AAM-B is capable of forming a hairpin loop in the phospholipid monolayer that surrounds the droplet.

Cell fractionation shows that AAM-B is targeted to droplets

Next we used cell fractionation to verify that AAM-B is targeted to droplets. COS7 cells were transfected with cDNA encoding the wild-type protein and the various mutant versions of AAM-B and grown overnight in media supplemented with 200 μM oleic acid. The cells were harvested and separated into droplet (LD), cytosol (Cyt) and total membrane (TM) fractions (Fig. 7B). Equal volumes of each fraction were separated by SDS-PAGE and processed for immunoblotting (Fig. 7C-F) to detect markers for cytosol (actin), ER (Bip, Sec61β, PDI) and droplets (ADRP). Coomassie Blue staining (Fig. 7B) showed that the amount of droplet protein loaded on gels was nearly undetectable, in contrast to the other fractions.

Immunoblots for ADRP, Bip, Sec61b, PDI and actin confirmed that the fractions were well separated. Wild-type AAM-B was detected in both the droplet and membrane fractions (Fig. 7C), although its specific activity in the droplet fraction was markedly higher. This dual localization is consistent with our immunofluorescence analysis showing some AAM-B in the ER (see Fig. 2B). Importantly, we did not detect any of the ER markers in the droplet fraction. The δN chimera was found exclusively in the membrane fraction (Fig. 7D). The C-terminal truncation of AAM-B (C6-myc) was only found in the droplet fraction (Fig. 7E). Finally, the ΔJxm mutant was restricted to the membrane fraction (Fig. 7F). These results are in complete agreement with the immunofluorescence experiments.

AAM-B interacts with itself

The aggregates of AAM-B in the cytoplasm that appeared when the N-terminus was deleted (Fig. 3E, N3) raise the possibility that full-length AAM-B forms oligomers. We used immunoprecipitation to detect AAM-B self-association. COS7 cells were co-transfected with cDNAs encoding HA-tagged wild-type AAM-B and either empty vector (Fig. 8A, lanes 1 and 3) or Myc-tagged wild-type

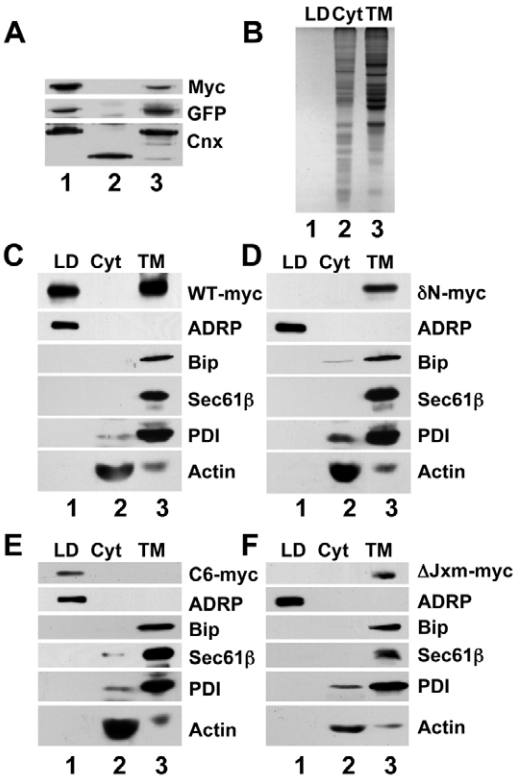

Fig. 7. Cell fractionation shows that AAM-B is targeted to droplets. (A) Protease-protection assay shows that AAM-B is exposed to the cytosol. HeLa cells were transfected with GFP-AAM-B-Myc and equal aliquots of the total membranes were incubated in the absence (lane 1) or presence (lanes 2 and 3) of trypsin. Lane 3 contained a protease inhibitor. An immunoblot for calnexin (Cnx) shows that the protein is reduced by ~10 kDa, which corresponds to the size of the cytosolic part of the protein. GFP and Myc are digested in the presence of trypsin, demonstrating that they are cytosolically oriented. (B-F) COS7 cells were transfected with cDNAs encoding Myc-tagged AAM-B constructs and cell fractions prepared. Equal volumes of the droplet, cytosol and membrane fractions were separated by SDS-PAGE. (B) A representative gel was stained with Coomassie Blue to determine the relative protein load for the immunoblots in C-F. (C-F) Each preparation was immunoblotted with α-Myc, α-ADRP, α-Bip, α-Sec61β, α-PDI and α-actin IgG. (C) The wild-type protein was found in both droplet and membrane fractions. (D) The δN mutant was found solely in the membrane fraction. (E) The C6 mutant was found in the droplet fraction. (F) The ΔJxm mutant was found in the membrane fraction.

AAM-B (lanes 2 and 4). The cells were lysed and processed to immunoprecipitate the Myc tag. The cleared lysate and the immunoprecipitate were processed for immunoblotting with α-HA IgG, α-Myc IgG and a pAb IgG against p63 (CKAP4), a transmembrane protein of the ER (Conrads et al., 2006; Mundy and Warren, 1992). AAM-B-Myc was not present in the cell lysate from cells expressing AAM-B-HA alone and, accordingly, the α-Myc IgG did not immunoprecipitate any AAM-B-Myc and AAM-B-HA was not detected in the immunoprecipitate (Fig. 8, lane 3). By contrast, in cells expressing both AAM-B-HA and AAM-B-Myc, the α-Myc IgG immunoprecipitated both AAM-B-Myc and AAM-B-HA (Fig. 8, lane 4), indicating that the two proteins were present in the same precipitate. p63 was detected in the lysates, but not in the immunoprecipitates, demonstrating that membranes were properly solubilized by the detergent. These results suggest that AAM-B can self-associate in the cell, which might be important for the functionality of the protein.

Another test for interaction is to see whether the wild-type AAM-B can recruit the normally cytosolic N3 AAM-B (Fig. 3D-F) to droplets (Fig. 8B-G). HeLa cells expressing either N3-AAM-B-Myc alone (Fig. 8B-D) or in combination with AAM-B-HA (Fig. 8E-G) were processed for immunofluorescence localization of the respective tags. N3-AAM-B-expressing cells stained with α-Myc had numerous aggregates throughout the cytoplasm (Fig. 8C) but no α-HA staining (Fig. 8B). By contrast, a subset of the cells (~5%) co-expressing N3-AAM-B and wild-type AAM-B showed nearly complete co-localization on the droplets (Fig. 8E-G). Although we are unsure why there was variability within each experiment, these results were reproducible in multiple trials. These results indicate that the soluble, truncated N3-AAM-B can interact with native AAM-B on the droplet.

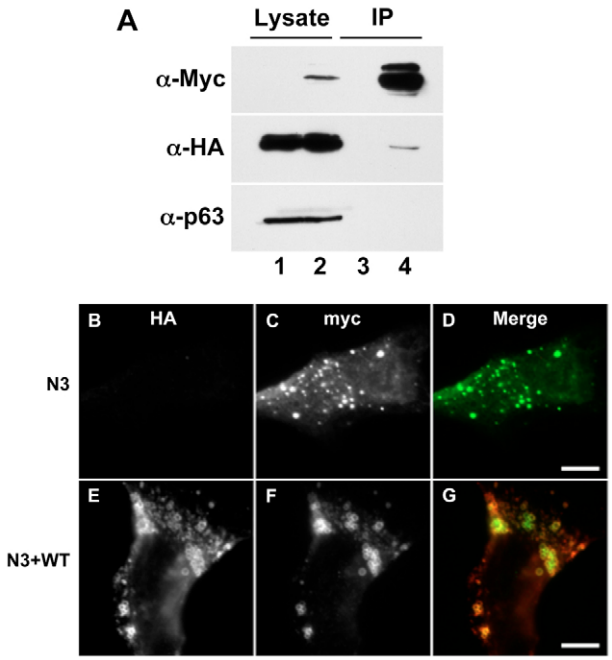

Fig. 8. AAM-B on droplets can interact with itself. (A) Co-immunoprecipitation of Myc-tagged and HA-tagged AAM-B co-expressed in HeLa cells. HeLa cells were co-transfected with cDNA encoding either HA-tagged AAM-B, Myc-tagged AAM-B (lanes 2 and 4) or empty vector (lanes 1 and 3). The cells were solubilized with detergent and processed to immunoprecipitate AAM-B-Myc with α-Myc IgG. Samples of the cleared cell lysates (lanes 1 and 2) and the immunoprecipitates (lanes 3 and 4) were separated by SDS-PAGE and immunoblotted with α-HA IgG, α-Myc IgG or α-p63 IgG. (B-G) Wild-type AAM-B can recruit truncated AAM-B from the cytoplasm to droplets. HeLa cells were co-transfected with a cDNA encoding Myc-tagged N3 and an empty vector (B-D). Cells were grown for 15 hours, fixed and processed for immunofluorescence detection of HA (B) and Myc (C). HeLa cells were co-transfected with a cDNA encoding Myc-tagged N3 and HA-tagged wild-type AAM-B (E-G). Cells were grown for 15 hours, fixed and processed for immunofluorescence detection of HA (E) and Myc (F). Scale bars: 5 μm.

To identify the region of AAM-B required for self-association, we co-expressed HA-tagged N4-AAM-B, which is missing amino acids 2-61, with C6-AAM-B, which lacks the C-terminus but is recruited to droplets (Fig. 4A-C). Expression of C6-AAM-B caused N4-AAM-B to localize in droplets (data not shown), which suggests that the methyltransferase domain mediates homotypic interaction of AAM-B within the droplet.

Discussion

We have identified a 28 amino acid hydrophobic motif that is responsible for targeting AAM-B to lipid droplets and can heterologously target proteins to this organelle (Fig. 4D-F; Fig. 5A-C). Including amino acids 29-39 with the first 28 amino acid stretch of AAM-B improves the efficiency of targeting (Fig. 4G-I), but is not required (Fig. 4J-L). In fact, various deletions and substitutions in the putative juxtamembrane region led to a loss of targeting in a somewhat unpredictable manner (Fig. 4A-C, supplementary material Fig. S1D-I). Thus, the juxtamembrane region might be important in stabilizing the 28 amino acid region, but does not appear to contain targeting information itself.

In addition to AAM-B, we identified similar N-terminal hydrophobic motifs in two other proteins (ALDI and CYB5R3) and found that each is sufficient to heterologously target proteins to droplets (Fig. 5A-F). There are other proteins in the droplet proteome with hydrophobic sequences at or near the N-terminus (Bartz et al., 2007) that might target in a similar mechanism. One of these proteins (asparagine-linked glycosylation 5 homolog) did not target to droplets (data not shown), nor did the N-terminal hydrophobic portion of CYP2C9. Since hydrophobicity alone is not sufficient, we speculate that a specific mechanism must exist for directing these proteins to the droplet.

Several droplet proteins have been identified that are inserted into droplets such that both the C- and N-terminal ends are in the cytoplasm (Zweytick et al., 2000). One such protein is oleosin, which depends on a proline knot in the middle of the molecule for targeting to plant lipid bodies (Abell et al., 1997). This type of topology might depend on the ability of the knot to form a hairpin loop in the membrane. We tested the possibility that the 1-28 AAM-B sequence might also be able to form a hairpin loop in the membrane by expressing a chimeric form of AAM-B that had GFP attached to the N-terminus and a Myc tag to the C-terminus. This molecule correctly targeted to droplets with both ends oriented towards the cytosol (Fig. 7A). It is formally possible, therefore, that 1-28 and related hydrophobic sequences target because they can form a hairpin in the droplet monolayer. The three sequences we identified that could target droplets all contained a central proline, perhaps aiding in hairpin orientation. Changing each proline to leucine, however, did not affect targeting. Either hairpin loops are not essential or there is another mechanism for achieving this topology.

A hairpin topology still does not explain why AAM-B concentrates in droplets. At low expression levels nearly all of the AAM-B is found on droplets, but when overexpressed we find it

in the ER too (Fig. 2B). If proteins like AAM-B were only passively permitted to reach regions were droplets form, they should be distributed between droplets and ER at all expression levels. This raises the possibility that droplets contain receptor-like molecules that attract AAM-B.

The ability of AAM-B to target yeast droplets indicates that the underlying molecular mechanism of targeting is common to all eukaryotic droplets. Our data suggest that the targeting process for this class of proteins involves co-translational insertion into the ER (Sakaguchi et al., 1984), lateral movement in the plane of the ER membrane, and delivery to droplets. A popular theory about how droplets form is that they bud from the cytosolic hemilayer of the ER into the cytoplasm of the cell. This model is attractive in the case of molecules like AAM-B because it appears to be adapted for monolayers. In fact, the targeting machinery might depend on the ability of 1-28 AAM-B to form a loop in the monolayer. The ability of AAM-B to self-associate does not appear to be required, either directly or indirectly, in targeting because multimer formation is dependent on the methyltransferase domain. The targeting machinery also has the ability to use molecules like AAM-B to drag interacting proteins from the cytoplasm or adjacent portions of the ER to the droplet. For example, co-expression of wild-type AAM-B with either cytosolic AAM-B N3 (Fig. 8B-G) or ER-located AAM-B δN (not shown) results in the relocation of each to the droplet. Therefore, AAM-B has the ability to recruit other proteins to the droplet. This raises the possibility that AAM-B and its relatives have crucial functions in organizing adiposome proteins that are important for the functionality of this organelle.

We do not believe that AAM-B is only incorporated into forming droplets because we found that AAM-B targets to endogenous droplets, not just those induced by feeding cells with oleic acid. It is possible, however, that droplets are constantly turning over, with small droplets budding from the ER and fusing with pre-existing droplets. Another possibility is that all droplets are in continuity with the ER. Thin-section and freeze-fracture electron microscopy have identified regions of apparent continuity between the phospholipid monolayer of the droplet and one of the bilayer leaflets of ER (Blanchette-Mackie et al., 1995), but it is not known whether all droplets are connected to ER. On the other hand, ER is often found associated with droplets (McGookey and Anderson, 1983) and this close apposition appears to be regulated by Rab18 (Martin et al., 2005; Ozeki et al., 2005). This raises the possibility that AAM-B is transferred from the ER to the droplet through transient contact sites between the two compartments. A precedent for this model is provided by mitochondrial-associated membrane (MAM), which comprises junction-like contact sites between ER and mitochondria that mediate the traffic of phosphatidylserine from ER to mitochondria for conversion to phosphatidylethanolamine (Vance, 2003). Finally, we cannot rule out the possibility that the delivery of AAM-B to droplets is mediated by vesicle traffic from the ER. In future work, identifying the mechanism of AAM-B traffic to droplets will have important implications for understanding how adiposomes package and distribute lipid droplets in the cell.

Materials and Methods

Materials

Taq DNA polymerase was from Takara Bio (Otsu, Shiga, Japan). Fugene 6 and Fugene HD were from Roche (Indianapolis, IN). mAb α-Myc (clone 9E10) - conjugated agarose beads, pAb α-HA and pAb α-Myc were from Santa Cruz Biotechnology (Santa Cruz, CA). pAb α-caveolin-1 and mAb α-Bip were from Becton Dickinson (Franklin Lakes, NJ). mAb α-Myc (clone 4A6) and pAb α-Sec61b were from Upstate Biotechnology (Charlottesville, VA). pAb α-protein disulfide isomerase IgG was from Stressgen Biotechnologies (San Diego, CA). mAb α-ADRP was from Fitzgerald Industries International (Concord, MA). Alexa Fluor-conjugated secondary antibodies, Bodipy 493/503 (D3922), HCS LipidTOX Red, pcDNA3.1 vectors and the CT GFP TOPO vector were from Invitrogen (Carlsbad, CA). The pAb α-GFP antibody was a kind gift from Joachim Seemann and the pAb α-p63 was a kind gift from Dorothy Mundy (both at U.T. Southwestern Medical Center at Dallas, TX). The HRP-conjugated α-mouse IgG was from Bio-Rad (Hercules, CA). Protease Inhibitor Cocktail Set III was from Calbiochem (San Diego, CA). Enhanced chemiluminescent (ECL) substrate was from Amersham (Piscataway, NJ). Sodium oleate, fetal bovine serum, mAb α-actin and DMEM were from Sigma (St Louis, MO). The Erg6-DsRed cDNA construct inserted between the PGK promoter and terminator in pRS315 vector, and the pRS316 vector carrying the PGK promoter and terminator were kind gifts from Joel Goodman (U.T. Southwestern Medical Center at Dallas, TX).

Cell culture

HeLa cells were cultured in DMEM (containing 4.5 g/l glucose) with 10% fetal bovine serum, 100 U/ml penicillin G and 100 mg/ml streptomycin sulfate. COS7 cells were cultured in similar media, but with 10% cosmic calf serum instead of fetal bovine serum. For microscopy experiments, HeLa cells were seeded to 12-well plates (50,000 cells per well) containing coverslips and grown overnight. For biochemical fractionation experiments COS7 cells were seeded to 15-cm dishes and grown overnight to ~80% confluence. For co-immunoprecipitation experiments, COS7 cells were seeded in 10-cm dishes and grown overnight. For quantification of wild-type AAM-B localization, HeLa cells were seeded in five 60-mm dishes (500,000 cells per dish) containing coverslips and grown overnight.

Cloning and mutagenesis

A cDNA containing the full-length coding sequence of human AAM-B was obtained from the RZPD (Berlin, Germany). A single coding point-mutation was corrected to match the published NCBI sequence (gi: 57283097) using the Stratagene (La Jolla, CA) QuikChange system. The cDNA was subcloned using PCR and the pGEM-T EZ TA cloning system (Promega, Madison, WI), incorporating 5′ *Xba*I and 3′ *Hin*dIII sites. The insert was excised using these sites and ligated into similarly restricted pcDNA3.1(–)Myc-His A. Deletions and alanine substitutions were introduced using the QuikChange system. To make the δN chimera, the coding region for cytochrome p450 2C9 was synthesized as two complimentary DNA oligos designed to carry ends that could be ligated to 5′ *Xba*I and 3′ *Eco*RI. The annealed oligos were ligated into pcDNA3.1(–)Myc-His A containing AAM-B nucleotides 85-732 inserted between *Eco*RI and *Hin*dIII. The C-terminal GFP fusion proteins were made by cloning PCR products into the CT-GFP TOPO vector. The N-terminal GFP fusion was made by primer extension overlap PCR. The chimeras joining CYB5R3 (gi: 4503327) nucleotides 1-84 and ALDI (gi: 27229118) nucleotides 1-81 to dominant-negative Rab5 were made by primer extension overlap PCR. The cDNA for human ADRP was obtained from the ATCC (Manasses, VA), restricted with *Eco*RI, gel-purified and ligated into *Eco*RI-digested pcDNA3.1(+)Myc-His A. The Myc tag was replaced with an HA tag on some constructs by restricting the vector with *Hin*dIII and *Afl*II and replacing the excised sequence with synthesized, annealed DNA oligos encoding the HA epitope. For insertion into pRS316, the cDNA for wild-type AAM-B was amplified using adaptamer primers that incorporated sequence homologous to the PGK promoter and terminator at the 5′ and 3′ ends of the PCR product, respectively. The PCR product was inserted into pRS316 carrying the PGK promoter and terminator by homologous recombination in yeast. All constructs were confirmed by sequencing using Applied Biosystems (ABI) Big Dye Terminator 3.1 chemistry and ABI capillary instruments.

Transfection and immunofluorescence

HeLa cells grown on coverslips in 12-well plates were transfected using Fugene 6 with 0.5 μg DNA per well according to the manufacturer's protocol. For co-expression studies, 0.25 μg of both cDNAs were used. In some experiments, transfected cells were grown for 15 hours and analyzed directly. In other experiments, transfected cells were first incubated at 37°C for 3-5 hours and then the medium was changed to complete HeLa medium containing 100 μM oleate (from a 100 mM stock in ethanol dissolved by sonication; final ethanol concentration 0.1%) and then incubated for 15 hours. The cells were washed twice with phosphate-buffered saline (PBS), fixed in 3% paraformaldehyde in PBS for 20 minutes at 24°C, and permeabilized with 0.1% (v/v) Triton X-100 in PBS for 5 minutes on ice. The coverslips were then processed for indirect immunofluorescence. The antibodies were diluted into PBS containing 1 mg/ml BSA: mAb α-Myc IgG (1:500), pAb α-HA IgG (1:300), pAb α-PDI IgG (1:100), and all Alexa-conjugated secondaries (1:500). In some cases the cells were stained for three minutes with Bodipy 493/503, diluted 1:100 from a 0.5 mg/ml stock in 1:1 ethanol:DMSO. For the yeast imaging, the BY4742 strain was co-transformed with wild-type AAM-B-GFP and Erg6-DsRed and spread on selective (uracil and leucine dropout) plates. Colonies were restreaked on selective plates twice. Yeast grown overnight in standard (2% glucose) dropout media were collected by centrifugation and prepared for fluorescence microscopy. Mammalian cells were viewed using a Zeiss (Oberkochen, Germany) Axioplan 2E fluorescence microscope

fitted with a Hamamatsu (Hamamatsu City, Japan) monochromatic digital camera. Images were acquired using OpenLab software (Improvision, Lexington, MA). Yeast cells were viewed with an Applied Precision (Seattle, WA) Deltavision RT deconvolution microscope. Images were captured and deconvolved using SoftWoRx software (Applied Precision, Issaquah, WA).

Biochemical fractionation

COS7 cells were grown to 80% confluence in 15-cm dishes and then transfected with 16.7 μg of the indicated cDNA using Fugene HD according to the manufacturer's protocol. Media were changed after 4 hours to media containing 100 μM oleate and the cells grown for an additional 15 hours. The cells were scraped into PBS containing 200 μM PMSF, centrifuged into a pellet and resuspended in 0.8 ml of Buffer A (250 mM sucrose, 20 mM tricine, pH 7.4) containing a protease inhibitor cocktail. The cells were incubated on ice for 20 minutes and then broken by five passes through a 22G1 needle. The lysates were centrifuged at 1000 ***g*** for 7 minutes. The post-nuclear supernatants (PNS) were layered over 300 μl Buffer B (500 mM sucrose, 20 mM Tris-HCl, pH 7.4) and centrifuged at 100,000 ***g*** for 30 minutes. The top 600 μl of the supernatant fraction, which contained the droplets, was collected into fresh tubes and concentrated by multiple rounds of centrifugation at 20,800 ***g*** for 3 minutes followed by removal of the underlying fraction using a gel-loading pipette tip. The underlying fraction was saved as cytosol. The Buffer B cushion was discarded. After the droplet samples were reduced to 100 μl, they were overlaid with 300 μl Buffer C (20 mM HEPES pH 7.4, 100 mM KCl, 2 mM $MgCl_2$) and centrifuged a final time. After the removal of 150 μl of the underlying fraction, the partially purified droplets were precipitated by the addition of 100% acetone. The membrane pellet was resuspended in 100 μl Buffer A by sonication. The protein concentration of the cytosol and membrane fractions was determined by the Bradford assay with a BSA standard and aliquots were then precipitated with acetone. The precipitated proteins were dissolved in sample buffer (62.5 mM Tris-HCl pH 6.8, 2% SDS, 25% glycerol, 0.01% Bromophenol Blue, 5% 2-mercaptoethanol) and boiled for 5 minutes. Equal fractions of the samples were separated on 10% SDS-PAGE gels and processed for immunoblotting.

Protease protection

COS7 cells in one 15-cm dish were transfected with cDNA encoding GFP-AAM-B using Fugene HD according to the manufacturer's protocol and were allowed to express overnight. The assay was conducted essentially as described previously (Espenshade et al., 1999). Briefly, cells were harvested and disrupted by ten passes through a ball-bearing homogenizer (10 μm clearance). Total membranes were collected by centrifugation for 15 minutes at 20,000 ***g***. The membranes were resuspended and divided into three aliquots: condition 1 was left untreated; conditions 2 and 3 were treated with 10 mg/ml trypsin; condition 3 contained benzamidine. The samples were incubated for 30 minutes at 30°C and the reactions were stopped by the addition of sample buffer followed by boiling. The samples were resolved by SDS-PAGE and processed for immunoblotting.

Co-immunoprecipitation experiments

Cells were grown in 10-cm dishes and each dish was transfected using Fugene HD with 6 μg HA-tagged AAM-B and either 6 μg Myc-tagged AAM-B or 6 μg empty vector, and cultured for an additional 15 hours. Unless noted, all subsequent steps were carried out at 4°C. The cells were washed twice in PBS and then solubilized in TETN (25 mM Tris-HCl, 5 mM EDTA, 150 mM NaCl, 1% Triton X-100, pH 7.5) containing a protease inhibitor cocktail, 1 ml per dish for 45 minutes. Lysates were centrifuged at 13,000 ***g*** for 10 minutes and the supernatants recovered to fresh tubes. Aliquots taken as input controls were precipitated by addition of 100% acetone and dissolved in SDS sample buffer. mAb α-Myc IgG conjugated to agarose beads was added to 1 mg of the cleared lysate and the samples rotated for 1 hour. The beads were then collected by centrifugation at 1000 ***g*** for 1 minute and washed four times with 1 ml of TETN containing protease inhibitors. After the final wash, the beads were resuspended in sample buffer, boiled for 5 minutes and separated on 12% SDS-PAGE gels. The gels were transferred to PVDF membranes and immunoblotted as previously described (Liu et al., 2004) using either pAb α-Myc (1:2000) or pAb α-HA (1:1000).

Quantification of wild-type AAM-B localization

HeLa cells grown in 60-mm dishes containing coverslips were transfected with 2 μg cDNA for AAM-B using Fugene 6 according to the manufacturer's protocol. The cells were cultured for 2, 4, 6, 8 or 23 hours before the coverslips were removed and processed for immunofluorescence. The remaining cells were scraped into PBS, collected by centrifugation and lysed in a small volume of PBS by probe sonication. The protein concentration of the lysate was measured and the remaining sample was processed for immunoblotting. The coverslips were scanned systematically and images taken of the first 50 transfected cells that were encountered. These images were then scored for the presence of droplet and ER staining patterns.

Sequence alignment

The first 23-28 amino acids of human AAM-B, mouse ALDI, human CYB5R3 and human CYP2C9 were aligned using ClustalW (Thompson et al., 1994).

We thank Charles Hall and Meifang Zhu for their valuable technical assistance; Brenda Pallares for administrative assistance; Drs Joel Goodman and Dirk Binns for valuable assistance and advice with the yeast droplet targeting experiments; and Dr Manu Hegde for pointing out the possible function of the proline residue in the droplet targeting sequences. This work was supported by grants from the National Institutes of Health, HL 20948, GM 52016, GM 70117, the Perot Family Foundation and the Cecil H. Green Distinguished Chair in Cellular and Molecular Biology.

References

Abell, B. M., Holbrook, L. A., Abenes, M., Murphy, D. J., Hills, M. J. and Moloney, M. M. (1997). Role of the proline knot motif in oleosin endoplasmic reticulum topology and oil body targeting. *Plant Cell* **9**, 1481-1493.

Bartz, R., Zehmer, J. K., Zhu, M., Chen, Y., Serrero, G., Zhao, Y. and Liu, P. (2007). Dynamic activity of lipid droplets: protein phosphorylation and Gtp-mediated protein translocation. *J. Proteome Res*. **6**, 3256-3265.

Binns, D., Januszewski, T., Chen, Y., Hill, J., Markin, V. S., Zhao, Y., Gilpin, C., Chapman, K. D., Anderson, R. G. and Goodman, J. M. (2006). An intimate collaboration between peroxisomes and lipid bodies. *J. Cell Biol*. **173**, 719-731.

Blanchette-Mackie, E. J., Dwyer, N. K., Barber, T., Coxey, R. A., Takeda, T., Rondinone, C. M., Theodorakis, J. L., Greenberg, A. S. and Londos, C. (1995). Perilipin is located on the surface layer of intracellular lipid droplets in adipocytes. *J. Lipid Res*. **36**, 1211-1226.

Bracey, M. H., Cravatt, B. F. and Stevens, R. C. (2004). Structural commonalities among integral membrane enzymes. *FEBS Lett*. **567**, 159-165.

Brasaemle, D. L., Dolios, G., Shapiro, L. and Wang, R. (2004). Proteomic analysis of proteins associated with lipid droplets of basal and lipolytically stimulated 3t3-L1 adipocytes. *J. Biol. Chem*. **279**, 46835-46842.

Conrads, T. P., Tocci, G. M., Hood, B. L., Zhang, C. O., Guo, L., Koch, K. R., Michejda, C. J., Veenstra, T. D. and Keay, S. K. (2006). Ckap4/P63 is a receptor for the Frizzled-8 protein-related antiproliferative factor from interstitial cystitis patients. *J. Biol. Chem*. **281**, 37836-37843.

Espenshade, P. J., Cheng, D., Goldstein, J. L. and Brown, M. S. (1999). Autocatalytic processing of Site-1 protease removes propeptide and permits cleavage of sterol regulatory element-binding proteins. *J. Biol. Chem*. **274**, 22795-22804.

Fujimoto, Y., Itabe, H., Sakai, J., Makita, M., Noda, J., Mori, M., Higashi, Y., Kojima, S. and Takano, T. (2004). Identification of major proteins in the lipid droplet-enriched fraction isolated from the human hepatocyte cell line Huh7. *Biochim. Biophys. Acta* **1644**, 47-59.

Hettema, E. H., Girzalsky, W., van Den Berg, M., Erdmann, R. and Distel, B. (2000). Saccharomyces cerevisiae Pex3P and Pex19P are required for proper localization and stability of peroxisomal membrane proteins. *EMBO J*. **19**, 223-233.

Hope, R. G., Murphy, D. J. and McLauchlan, J. (2002). The domains required to direct core proteins of hepatitis C virus and GB virus-B to lipid droplets share features with plant oleosin proteins. *J. Biol. Chem.* **277**, 4261-4270.

Huh, W. K., Falvo, J. V., Gerke, L. C., Carroll, A. S., Howson, R. W., Weissman, J. S. and O'Shea, E. K. (2003). Global analysis of protein localization in budding yeast. *Nature* **425**, 686-691.

Litvak, V., Shaul, Y. D., Shulewitz, M., Amarilio, R., Carmon, S. and Lev, S. (2002). Targeting of Nir2 to lipid droplets is regulated by a specific threonine residue within its pi-transfer domain. *Curr. Biol*. **12**, 1513-1518.

Litvak, V., Dahan, N., Ramachandran, S., Sabanay, H. and Lev, S. (2005). Maintenance of the diacylglycerol level in the Golgi apparatus by the Nir2 protein is critical for Golgi secretory function. *Nat. Cell Biol*. **7**, 225-234.

Liu, P., Ying, Y., Zhao, Y., Mundy, D. I., Zhu, M. and Anderson, R. G. (2004). Chinese hamster ovary K2 cell lipid droplets appear to be metabolic organelles involved in membrane traffic. *J. Biol. Chem*. **279**, 3787-3792.

Liu, P., Bartz, R., Zehmer, J. K., Ying, Y. S., Zhu, M., Serrero, G. and Anderson, R. G. (2007). Rab-regulated interaction of early endosomes with lipid droplets. *Biochim. Biophys. Acta* **1773**, 784-793.

Marchler-Bauer, A. and Bryant, S. H. (2004). Cd-Search: protein domain annotations on the fly. *Nucleic Acids Res*. **32**, W327-W331.

Martin, S., Driessen, K., Nixon, S. J., Zerial, M. and Parton, R. G. (2005). Regulated localization of Rab18 to lipid droplets: effects of lipolytic stimulation and inhibition of lipid droplet catabolism. *J. Biol. Chem.* **280**, 42325-42335.

McGookey, D. J. and Anderson, R. G. (1983). Morphological characterization of the cholesteryl ester cycle in cultured mouse macrophage foam cells. *J. Cell Biol*. **97**, 1156-1168.

McManaman, J. L., Zabaronick, W., Schaack, J. and Orlicky, D. J. (2003). Lipid droplet targeting domains of adipophilin. *J. Lipid Res*. **44**, 668-673.

Mullner, H., Zweytick, D., Leber, R., Turnowsky, F. and Daum, G. (2004). Targeting of proteins involved in sterol biosynthesis to lipid particles of the yeast Saccharomyces cerevisiae. *Biochim. Biophys. Acta* **1663**, 9-13.

Mundy, D. I. and Warren, G. (1992). Mitosis and inhibition of intracellular transport stimulate palmitoylation of a 62-Kd protein. *J. Cell Biol*. **116**, 135-146.

Murphy, D. J. (2001). The biogenesis and functions of lipid bodies in animals, plants and microorganisms. *Prog. Lipid Res*. **40**, 325-438.

Ohsaki, Y., Maeda, T., Maeda, M., Tauchi-Sato, K. and Fujimoto, T. (2006). Recruitment of Tip47 to lipid droplets is controlled by the putative hydrophobic cleft. *Biochem. Biophys. Res. Commun*. **347**, 279-287.

Ostermeyer, A. G., Paci, J. M., Zeng, Y., Lublin, D. M., Munro, S. and Brown, D. A. (2001). Accumulation of caveolin in the endoplasmic reticulum redirects the protein to lipid storage droplets. *J. Cell Biol*. **152**, 1071-1078.

Ozeki, S., Cheng, J., Tauchi-Sato, K., Hatano, N., Taniguchi, H. and Fujimoto, T. (2005). Rab18 Localizes to lipid droplets and induces their close apposition to the endoplasmic reticulum-derived membrane. *J. Cell Sci.* **118**, 2601-2611.

Sakaguchi, M., Mihara, K. and Sato, R. (1984). Signal recognition particle is required for co-translational insertion of cytochrome P-450 into microsomal membranes. *Proc. Natl. Acad. Sci. USA* **81**, 3361-3364.

Subramanian, V., Garcia, A., Sekowski, A. and Brasaemle, D. L. (2004). Hydrophobic sequences target and anchor perilipin a to lipid droplets. *J. Lipid Res.* **45**, 1983-1991.

Thompson, J. D., Higgins, D. G. and Gibson, T. J. (1994). CLUSTAL W: improving the sensitivity of progressive multiple sequence alignment through sequence weighting, position-specific gap penalties and weight matrix choice. *Nucleic Acids Res.* **22**, 4673-4680.

Turro, S., Ingelmo-Torres, M., Estanyol, J. M., Tebar, F., Fernandez, M. A., Albor, C. V., Gaus, K., Grewal, T., Enrich, C. and Pol, A. (2006). Identification and characterization of associated with lipid droplet protein **1**, a novel membrane-associated protein that resides on hepatic lipid droplets. *Traffic* **7**, 1254-1269.

Umlauf, E., Csaszar, E., Moertelmaier, M., Schuetz, G. J., Parton, R. G. and Prohaska, R. (2004). Association of stomatin with lipid bodies. *J. Biol. Chem*. **279**, 23699-23709.

van Meer, G. (2001). Caveolin, cholesterol, and lipid droplets? *J. Cell Biol.* **152**, F29-F34.

Vance, J. E. (2003). Molecular and cell biology of phosphatidylserine and phosphatidylethanolamine metabolism. *Prog. Nucleic Acid Res. Mol. Biol*. **75**, 69-111.

Zweytick, D., Athenstaedt, K. and Daum, G. (2000). Intracellular lipid particles of eukaryotic cells. *Biochim. Biophys. Acta* **1469**, 101-120.